doi: 10.4149/gpb_2025025

lncRNA H19 contributes to sevoflurane-induced neuronal death in SH-SY5Y cells *via* ACSL4-mediated ferroptosis pathway

Lixin Liu[1], Zhaoping Xue[1], Yan Liu[2] and Ying Liu[2]

[1] *Department of Anesthesia Recovery Room, The First Hospital of Jilin University, Changchun, China*
[2] *Department of Spinal Surgery, The First Hospital of Jilin University, Changchun, China*

Abstract. Sevoflurane induces neurotoxicity and cognitive impairment, with long noncoding RNAs (lncRNAs) playing key roles in nervous system diseases. This study explored lncRNA H19's function in sevoflurane-induced neurotoxicity. SH-SY5Y cell viability and apoptosis were assessed *via* CCK8 and TUNEL assays. Gene expression was measured by RT-qPCR, while reactive oxygen species (ROS), malondialdehyde (MDA), glutathione (GSH), and iron levels were quantified. Subcellular fractionation determined H19 localization, and luciferase assays confirmed H19/miR-20a-5p and miR-20a-5p/Acyl-CoA synthetase long chain family member 4 (ACSL4) interactions. Western blot analyzed ACSL4, apoptosis-, and ferroptosis-related proteins. The results showed that sevoflurane reduced viability, promoted apoptosis and ferroptosis, and upregulated H19 and ACSL4. H19 knockdown mitigated neurotoxicity by restoring viability, GSH, solute carrier family 7 member 11 (SLC7A11), and glutathione peroxidase 4 (GPX4), while reducing apoptosis, MDA, ROS, and iron. Mechanistically, H19 sponged miR-20a-5p to elevate ACSL4. Rescue assays showed miR-20a-5p inhibition or ACSL4 overexpression reversed H19 silencing's protective effects. Thus, H19 depletion alleviates sevoflurane-induced neuronal damage *via* the miR-20a-5p/ACSL4 axis, suggesting a potential therapeutic target.

Key words: Long noncoding RNA H19 — Ferroptosis — Sevoflurane — ACSL4

Introduction

As one of the most common anesthetics, sevoflurane is always applied in clinical operations (Qiu et al. 2016; Wang et al. 2016). Studies have illuminated that improper or excessive inhalation of sevoflurane can bring about impaired learning and memory abilities (Kodama et al. 2011; Lai et al. 2016). Apoptosis (Dong et al. 2009), inflammation (Sánchez-Conde et al. 2008), and neurodevelopment repression (Zhu et al. 2017) occurring after exposure to high concentrations (3–4%) of sevoflurane lead to long-term cognitive disorder (Le Freche et al. 2012; Tian et al. 2015). Recently, ferroptosis has been identified as non-apoptotic cell death process in nervous system diseases involving accumulation of reactive oxygen species (ROS) and lipid peroxide as well as iron overload (Hirschhorn and Stockwell 2019; Wu et al. 2019). Ferroptosis is also accompanied by alterations in malondialdehyde (MDA) and glutathione (GSH) (Chen et al. 2021). It has been reported that sevoflurane stimulation results in cognitive impairment without affecting neuro-apoptosis, suggesting that sevoflurane-caused cognitive dysfunction may be induced by other cell death mechanisms (Lu et al. 2016). It is worth noting that iron metabolism disorder has been shown to be highly related to the pathogenesis of anesthetics, including neurological deficits and neurotoxicity induced by sevoflurane exposure (Zuo et al. 2021). Reports of studies on rodents disclose that cognitive dysfunction can be resulted from the overloaded iron by iron homeostasis disruption as a result from general anesthesia including

Correspondence to: Ying Liu, Department of Spinal Surgery, The First Hospital of Jilin University, No. 1, Xinmin Street, Changchun 130021, China
E-mail: ly1116@jlu.edu.cn

© The Authors 2026. This is an **open access** article under the terms of the Creative Commons Attribution-NonCommercial 4.0 International License (https://creativecommons.org/licenses/by-nc/4.0/), which permits non-commercial use, distribution, and reproduction in any medium, provided the original work is properly cited.

sevoflurane and ketamine (Wu 2020). Nevertheless, the mechanisms by which sevoflurane induces ferroptotic neuron death deserve further exploration.

Numerous long noncoding RNAs (lncRNAs) and their critical functions have been recognized in a variety of diseases, including neurodegenerative diseases, which thus has attracted extensive attention in recent years (Ramos et al. 2013; Liu and Li 2020). lncRNAs are a category of noncoding RNAs (>200 nt), which can elicit pivotal functions in the regulation of various pathological and physiological processes by playing as an endogenous competitive RNA (ceRNA) competing for microRNAs (miRNAs) against messenger RNAs (mRNAs) (Pouyanrad et al. 2019; Dieter et al. 2020; Zhang B et al. 2020). Dysregulation of lncRNAs has been implicated in the development of multiple neurodegenerative diseases such as epilepsy, Alzheimer's disease (AD), and Parkinson's disease. For example, lncRNA UCA1 suppresses seizure-evoked brain injury and epilepsy *via* regulation of the miR-495/Nrf2-ARE pathway (Geng et al. 2018). Reduced lncRNA MAGI2-AS3 inhibits neuroinflammation and neurotoxicity caused by amyloid-β induction *via* targeting miR-374b-5p/BACE1 axis in Alzheimer's disease cell model (Zhang and Wang 2021). H19 is a highly expressed lncRNA in intracerebral hemorrhage (Kim et al. 2019), which exerts essential functions in the modulation of apoptosis, cellular proliferation, inflammation, lipid metabolism, adipocyte differentiation, and angiogenesis (Shi et al. 2020). It is noteworthy that the important role of H19 in the nervous system has been reported in recent studies. A report shows that H19 contributes to ferroptosis in brain microvascular endothelial cells (BMVECs) by upregulating Acyl-CoA synthetase long chain family member 4 (ACSL4) expression (Chen et al. 2021). Another report reveals that H19 silencing lowers the expression of GPX4, which is a key regulator of ferroptosis, in spontaneous abortion. In addition, silenced H19 also suppresses Bcl-2 expression while increases Bax expression in HTR-8 cells (Bai and Tang 2021). Additionally, downregulated H19 attenuates neuropathic pain by suppressing inflammatory responses in chronic constriction injury-induced rat models *in vivo* (Meng et al. 2022). Moreover, H19 depletion protects against isoflurane-induced cognitive dysregulation by repressing neuroinflammation (Ge et al. 2022). However, whether H19 is involved in ferroptosis in sevoflurane-induced neurons remains completely unknown.

ACSL4 is a member of the long chain acyl coenzyme A synthase family, which functions as a key enzyme controlling fatty acid metabolism (Kuwata and Hara 2019). The synthesis of acyl-CoA from fatty acids, which is the main process linked to ferroptosis, can be catalyzed by ACSL4 (Doll et al. 2017). As an essential modulator of ferroptosis, enhanced ACSL4 expression activates the ferroptosis pathway (Yuan et al. 2016; Kagan et al. 2017), while ACSL4 deficiency facilitates glioma cell proliferation *via* inhibition of ferroptosis (Cheng et al. 2020). Moreover, inhibited ACSL4 has been shown to attenuate neuroinflammation and brain damage caused by ferromyopathy (Cui et al. 2021). Notably, H19 is demonstrated to play as a ceRNA to modulate the ferroptosis and proliferation of BMVECs by targeting the miR-106b-5p/ACSL4 axis (Chen et al. 2021). Nevertheless, whether H19 plays as a ceRNA to regulate ACSL4 in sevoflurane-induced neurons has not been elucidated yet.

In this study, we used the human neuroblastoma cell line SH-SY5Y to investigate the functional role and molecular mechanism by which H19 regulates sevoflurane-induced neurotoxicity. We hypothesized that H19 may upregulate ACSL4 to promote sevoflurane-induced neuronal death in SH-SY5Y cells *via* activating the ferroptosis pathway.

Materials and Methods

Cell culture

American type culture collection (Manassas, VA, USA)-provided human neuroblastoma cell line (SH-SY5Y; CRL-2266) were cultured in Dulbecco's modified Eagle medium (DMEM) basal culture medium (0001, iCell Bioscience Inc., Shanghai, China) supplemented with 10% fetal bovine serum (FBS; 76294-180, AVANTOR, Australia) under the atmosphere of 95% air/5% CO_2 at 37°C.

Cell transfection

Short hairpin RNAs antagonistic to H19 (sh-H19#1/2) and scrambled negative control (sh-NC) were synthesized by GenePharma (Shanghai, China). miR-20a-5p mimics (miR-20a-5p), miR-20a-5p inhibitor, and scrambled oligomer sequences (miR-NC and NC inhibitor) were purchased from Sangon Biotech (Shanghai, China). The pcDNA3.1 vector (Invitrogen Inc., Carlsbad, CA, USA) inserted with the amplified cDNA sequence of ACSL4 was used to create ACSL4-overexpressing plasmid (ACSL4) with the empty pcDNA3.1 vector (Vector) as the negative control. Once reaching 80% confluence, the abovementioned oligonucleotides diluted at a final concentration of 20 μM were transfected into SH-SY5Y cells (1×10^5/ml) on six-well plates in the presence of Lipofectamine® 3000 reagent (L3000-015, Invitrogen), followed by exposure of SH-SY5Y cells to 4.1% sevoflurane (orb62837, Biorbyt, Booute biotechnology Co., Ltd., Wuhan, China) for 6 h.

Cell Counting Kit-8 (CCK-8) assay

According to the product manual, CCK-8 assay was performed to evaluate the viability of SH-SY5Y cells. Briefly,

SH-SY5Y cells (1×10^5) inoculated on the 96-well plates were subjected to transfection and/or 4.1% sevoflurane stimulation. Then, 10 μl CCK-8 solution (Solarbio, Beijing, China) was added into each well of the plate for a 4-h incubation with SHSY5Y cells at 37°C. Cell viability was tested *via* determination of the optical density at 450 nm using a microplate reader (Bio-Rad Laboratories, Hercules, CA, USA).

Western blot analysis

Total protein was isolated by disrupting SH-SY5Y cells using RIPA buffer (PH0316, PHYGENE, Fuzhou, China), followed by quantification using the bicinchoninic acid (BCA) method (E112-01, Vazyme, Nanjing, China). Constant pressure electrophoresis was implemented at 80 V after adding concentrated adhesives and separate adhesives into the electrophoretic splint. The PVDF membrane was soaked by pure methanol. Prior to tightening the splint, the transfer device was assembled following the steps: sponge → layer filter paper → glue → film → layer filter paper → sponge. The transfer tank was added with transfer buffer following being placed in an ice bath and then on the sandwich deck. After inserting the electrode, the membrane was sealed in 25 ml 5% non-fat milk powder buffer for 60 min and then rinsed by TBS/T trice with 5 min each time. Primary antibodies against Bax (ab182734, 1:1,000, Abcam), GPX4 (ab125066, 1:5,000, Abcam), Bcl-2 (ab196495, 1:2,000, Abcam), ACSL4 (ab155282, 1:10,000, Abcam), SLC7A11 (ab216876, 1:1,000, Abcam), and GAPDH (ab125247, 1:5,000, Abcam) were added for overnight-incubation with the membrane at 4°C. After another washing with TBS/T three times, the membrane was processed by 1-h incubation with secondary antibody (ab96899, 1:10000) at 37°C. GAPDH functioned as the loading control. Electrochemiluminescence system (Thermo Fisher Scientific) was used to visualize the protein bands that were quantified with the ImageJ software (National Institutes of Health).

Real time-quantitative polymerase chain reaction (RT-qPCR) analysis

The levels of mRNA and miRNA were measured using RT-qPCR. Total RNA was extracted by mixing SH-SY5Y cells with TRIzol reagent (Invitrogen). RT was executed as instructed by the TaqMan MiRNA (Applied Biosystems) RT kit, and TaqMan miRNA assay (Applied Biosystems) was used to quantify miR-323a-3p with U6 as its internal reference. Reverse transcription of mRNA to cDNA was achieved using PrimeScript Strand cDNA synthesis kit (Takara, Japan). RT-qPCR was implemented with SYBR Premix Ex Taq II (Takara) for the evaluation of mRNA levels with GAPDH as its internal control. The Applied Biosystems 7900HT Fast Real-Time PCR System (Applied Biosystems) was adopted for all RT-qPCR analysis with $2^{-\Delta\Delta Ct}$ method for the quantification of relative gene expression. The sequences of primers are presented in Table 1.

Table 1. Primer sequences used for RT-qPCR

Gene	Primer sequence (5′–3′)
H19	F: CGCTTTTGAACCAGCAGGG
	R: TTCCCGAGGCTTTGGTGTG
miR-20a-5p	F: GTAAAGTGCTTATAGTGCAG
	R: GTCGTATCCAGTGCGTGTCG
ACSL4	F: TATTCTTCTCCGCTTACACTCTCTG
	R: TATAATTCATCTCTTGGACTTTGCTC
GAPDH	F: TTGGTATCGTGGAAGGACTCA
	R: TGTCATCATATTTGGCAGGTT
U6	F: CTCGCTTCGGCAGCACA
	R: AACGCTTCACGAATTTGCGT

F, forward; R, reversed.

Measurement of MDA, GSH, and iron levels

The levels of MDA, GSH, and iron were examined using the intracellular Lipid Peroxidation MDA Assay Kit (AAT-B15991, AAT Bioquest, USA), intracellular GSH Assay Kit (orb511104, biorbyt), and Iron Assay Kit (KA1647, Abnova, Shanghai Qunji Biotech Co., Ltd., Shanghai, China) as *per* the manufacturer's directions.

Subcellular fraction assay

Approximately 1×10^7 SHSY5Y cells were collected for the separation of cytoplasmic and nuclear RNA utilizing the PARIS Kit (Invitrogen). By the means of RT-qPCR, H19 expression distribution in SHSY5Y cells was determined by analyzing the cytoplasmic and nuclear fractions. GAPDH functioned as cytoplasmic control while U6 served as the nuclear control.

TdT-mediated dUTP nick-end labeling (TUNEL) assay

Cells were cultured overnight following transfection and/or sevoflurane stimulation. Then, PBS was employed for twice rinsing of the cells that were subjected to fixation in 4% paraformaldehyde for 15 min. Prior to permeabilization in 0.25% Triton-X 100 for 20 min, the cells were washed by PBS again. With the employment of 50 μl TUNEL solution (Beyotime Biotechnology, China) for staining, the positively labeled nuclear cells were denoted as apoptotic cells. The images of positive cells in six random views were captured under a fluorescence microscope (Nikon, Japan). The percentage of TUNEL positive cells was calculated as positive cells/total cells.

Detection of ROS level

A dichlorofluorescin diacetate (DCFDA) Cellular ROS Assay Kit (ab113851, Abcam Inc., Cambridge, UK) was used to stain SH-SY5Y cells for detecting ROS generation. As instructed by the product directions, cells plated on 96-well plates were rinsed once with kit-provided buffer and then stained with DCFDA in darkness at room temperature for 45 min. After rinsing again with buffer, a fluorescent microscope (Nikon, Japan) or microplate reader (Bio-Rad Laboratories) was utilized for the analyzation of ROS generation.

Luciferase reporter assay

Potential targets of miR-20a-5p were predicted utilizing TargetScan (https://www.targetscan.org/vert_72/) and ENCORI (https://starbase.sysu.edu.cn/). The human H19 3′UTR containing a putative miR-20a-5p binding site and its mutated version generated by changing seven complementary nucleotides GCACUUU in the binding site to CGUGAAA were inserted into the luciferase reporter vector pmirGLO to construct H19-Wt and H19-Mut. Similarly, ACSL4-Wt and ACSL4-Mut were constructed by inserting ACSL4 3′UTR harboring a putative miR-20a-5p binding site and its mu-

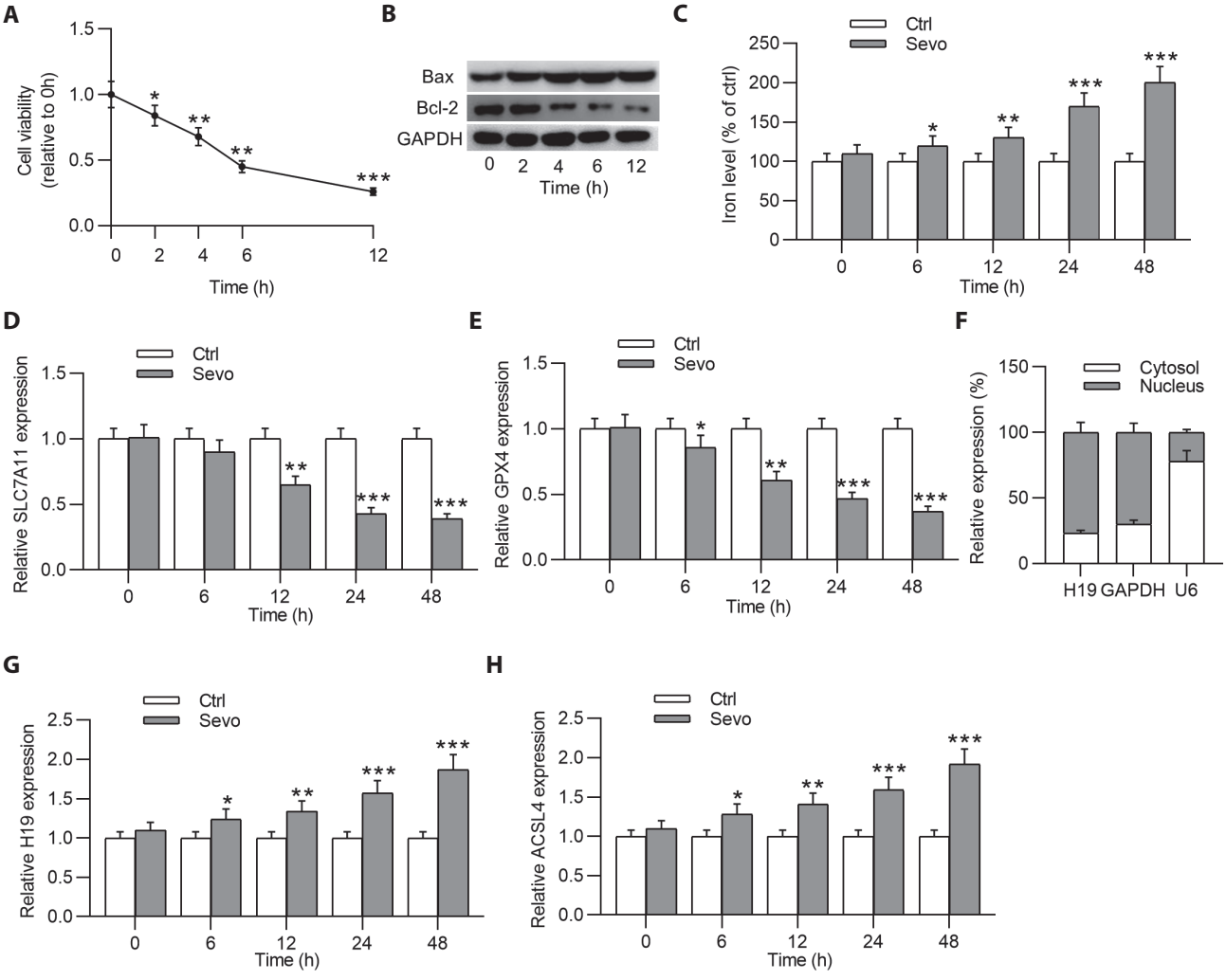


Figure 1. Effects of sevoflurane on H19 and ACSL4 expression and SH-SY5Y cells. After exposing SH-SY5Y cells to 4.1% sevoflurane for 0, 2, 4, 6, and 12 h, cell viability and apoptosis-related genes (Bax and Bcl-2) were detected by CCK-8 assay (**A**) and Western blot analysis (**B**). **C.** Iron level was measured by commercial kits at 0, 6, 12, 24, and 48 h following sevoflurane treatment. SLC7L11 (**D**) and GPX4 (**E**) expression was examined at 0, 6, 12, 24, and 48 h after sevoflurane stimulation using RT-qPCR analysis. **F.** The distribution of H19 was determined by subcellular fractionation assay. H19 (**G**) and ACSL4 (**H**) expression at 0, 6, 12, 24, and 48 h after sevoflurane exposure by RT-qPCR. Measurement data are expressed as mean ± SD. * $p < 0.05$, ** $p < 0.01$, *** $p < 0.001$. Sevo, sevoflurane; Ctrl, Control.

tated version into the luciferase reporter vector pmirGLO. SH-SY5Y cells plated in 24-well plates were co-transfected with 100 ng vectors and miR-NC or miR-20a-5p utilizing Lipofectamine® 3000 (Invitrogen) according to the supplier's instructions. The alterations of fluorescence intensity were assessed *via* the Luciferase Reporter Assay System (Promega, Madison, WI, USA).

Statistical analysis

Measurement data from at least three independent experiments are expressed as the mean ± standard deviation (SD). GraphPad Prism 7.0 software (GraphPad Software Inc., La Jolla, CA, USA) was used to perform statistical analysis. Experimental data were compared using Student's *t*-test (2 groups) and one-way analysis of variance (ANOVA) followed by Tukey's *post hoc* tests (>2 groups). Any *p* value less than 0.05 was considered statistically significant.

Results

Sevoflurane upregulates H19 and ACSL4 expression and induces SH-SY5Y cell death

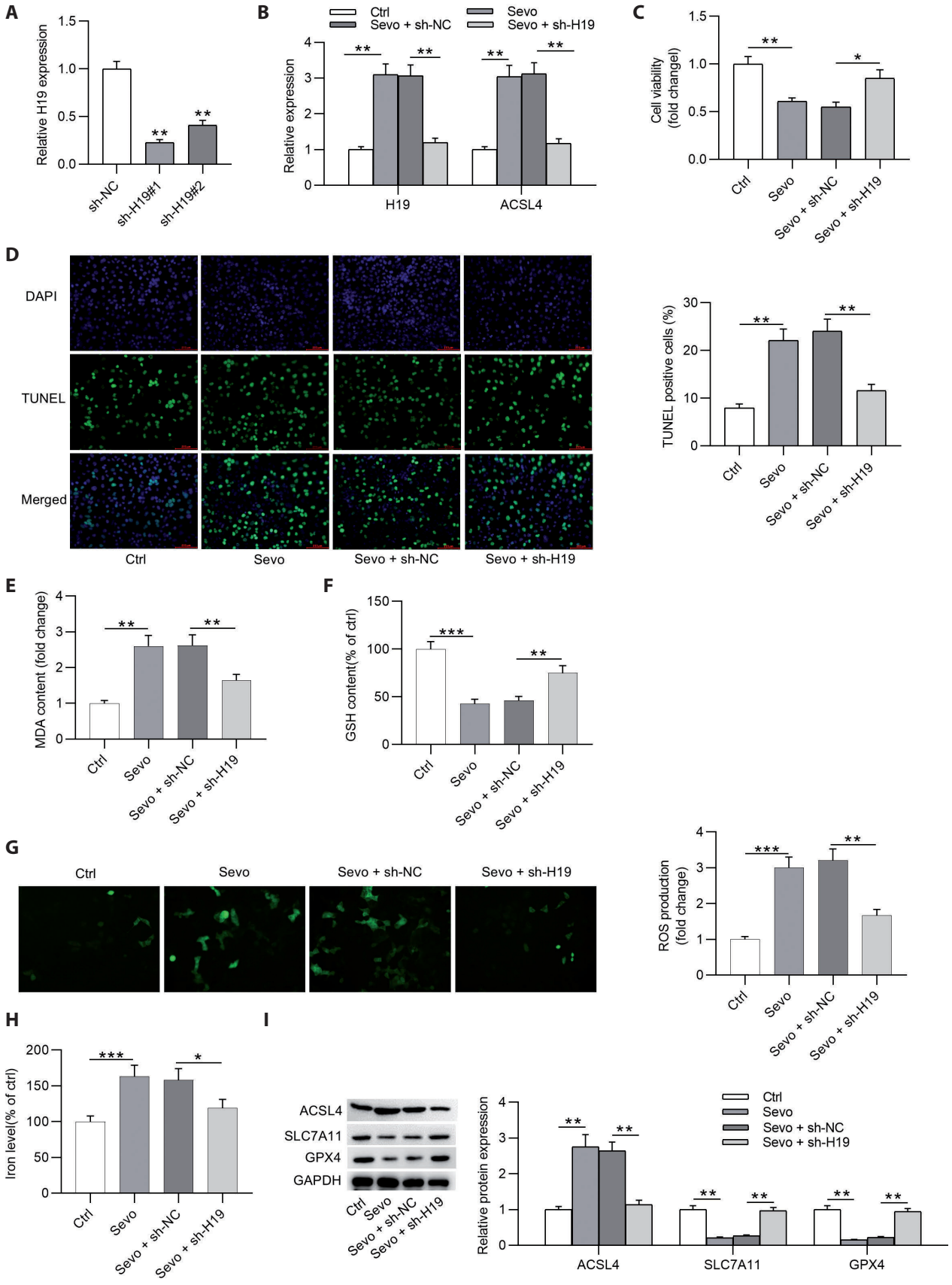
To investigate the effect of sevoflurane on neurons, SH-SY5Y cells were treated with 4.1% sevoflurane for 0, 2, 4, 6, or 12 h. CCK-8 results described that SH-SY5Y cell viability was time-dependently suppressed by sevoflurane management (Fig. 1A). Sevoflurane also increased Bax expression while decreased Bcl-2 expression in a time-dependent manner (Fig. 1B), which suggested that sevoflurane triggers neuronal damage in SH-SY5Y cells. Then, the level of iron and the expression of SLC7A11 and GPX4, which are iron death-correlated genes, were detected at 0, 6, 12, 24 and 48 h post sevoflurane treatment. As a result, iron level was significantly increased in sevoflurane-treated cells *versus* control cells absent from sevoflurane management (Fig. 1C). Meanwhile, SH-SY5Y cells treated with 4.1% sevoflurane displayed significantly lower SLC7A11 expression at 12, 24 and 48 h and GPX4 expression at 6, 12, 24 and 48 h than control cells (Fig. 1D,E). These findings indicated that ferroptosis is involved in sevoflurane-induced SH-SY5Y cell damage. It has been reported that the biological functions of lncRNAs are largely dependent on their cellular location (Liu and Wu 2020). Therefore, we explored the localization of H19 in SH-SY5Y cells, where H19 was mainly localized in the cytoplasm (Fig. 1F). In addition, it was found that the expression of H19 and ACSL4 was notably elevated at 6, 12, 24 and 48 h after sevoflurane exposure compared with the control group (Fig. 1G,H). Therefore, we concluded that sevoflurane induces SH-SY5Y cell death and elevates H19 and ACSL4 expression.

Reduced H19 ameliorates sevoflurane-induced neuronal damage by suppressing ACSL4

It has been demonstrated that H19 promotes ferroptosis in BMVECs by elevating ACSL4 (Chen et al. 2021). Inhibition of ACSL4 suppresses sevoflurane-induced ferroptotic neuronal death in SH-SY5Y cells (Cheng et al. 2021). Thus, we hypothesized that H19 may attenuate sevoflurane-caused neuronal injury *via* downregulation of ACSL4. To validate our hypothesis, H19 expression was first silenced by transfecting sh-H19#1/2 into SH-SY5Y cells and successful knockdown efficiency was confirmed by RT-qPCR (Fig. 2A). Since SH-SY5Y cells expressed lower H19 expression after sh-H19#1 transfection, sh-H19#1 denoted as sh-H19 was selected for subsequent experiments. As shown in Figure 2B, sevoflurane-induced elevation of H19 expression was reversed by silenced H19. Consistently, ACSL4 expression upregulated in sevoflurane-treated cells was reduced upon H19 depletion. To probe into the role of H19 in sevoflurane-generated neuronal damage, SH-SY5Y cells were transfected with sh-H19 and incubated for 24 h, followed by treatment with 4.1% sevoflurane for 6 h. Functional assays revealed that silencing of H19 significantly eliminated sevoflurane-evoked suppression on SH-SY5Y cell viability (Fig. 2C). Accordingly, there was an increase in the percent of TUNEL positive cells caused by sevoflurane induction, which was reversed upon H19 suppression (Fig. 2D). Additionally, sevoflurane treatment brought about an increase in MDA content, a decrease in GSH content and upregulations in ROS production and iron level, and these effects were abrogated after sh-H19 transfection (Fig. 2E–H). Furthermore, the protein expression of ACSL4 was increased whereas the expression of SLC7A11and GPX4 was decreased following sevoflurane stimulation. However, sevoflurane administration-induced effects on these proteins were restored by silenced H19 (Fig. 2I). Taken together, inhibition of H19 mitigates sevoflurane-induced SH-SY5Y cell death *via* reduction of ASCL4.

H19 targets ACSL4 via sponging miR-20a-5p

It is widely reported that lncRNAs that primarily distributed in the cytoplasm can play as ceRNAs to complete for miRNAs against mRNA (Ma 2020). To develop the mechanism by which H19 regulating sevoflurane-generated neurotoxicity, ENCORI together with TargetScan databases were searched to predicate the potential miRNAs for H19 and ACSL4, and 17 candidate miRNAs were identified (Fig. 3A). RT-qPCR analysis illuminated that the most significantly reduced miRNA in SH-SY5Y cells responding to sevoflurane administration was hsa-miR-20a-5p (Fig. 3B). Thus, we deduced that miR-20a-5p was a target for H19. To validate the possibility that miR-20a-5p could directly interact with H19 and ACSL4, miR-20a-5p expression was upregulated


A
Relative H19 expression
sh-NC
sh-H19#1
sh-H19#2
B
Ctrl
Sevo + sh-NC
Sevo
Sevo + sh-H19
Relative expression
H19
ACSL4
C
Cell viability (fold change)
Ctrl
Sevo
Sevo + sh-NC
Sevo + sh-H19
D
DAPI
TUNEL
Merged
Ctrl
Sevo
Sevo + sh-NC
Sevo + sh-H19
TUNEL positive cells (%)
E
MDA content (fold change)
F
GSH content(% of ctrl)
G
ROS production (fold change)
H
Iron level(% of ctrl)
I
ACSL4
SLC7A11
GPX4
GAPDH
Relative protein expression

◂ **Figure 2.** Suppression of H19 attenuates sevoflurane-induced neuronal damage by reducing ACSL4. **A.** The knockdown efficiency of H19 by RT-qPCR. **B.** SH-SY5Y cells were stimulated by sevoflurane alone or transfected with sh-NC or sh-H19 followed by administration with sevoflurane for 6 h. The expression of H19 and ACSL4 in Ctrl, Sevo, Sevo+sh-NC, and Sevo+sh-H19 groups was detected by RT-qPCR. **C.** Cell viability in each group was evaluated by performing CCK-8 assay. **D.** The percentage of TUNEL positive cells in each group. Commercial kits examined the contents of MDA (**E**) and GSH (**F**) in the indicated groups. **G.** ROS content was tested by DCFDA staining assay. **H.** Iron level by commercial kits. **I.** The protein intensity and quantification of ACSL4, SLC7A11, and GPX4 in Ctrl, Sevo, Sevo+sh-NC, and Sevo+sh-H19 groups by Western blot analysis. Measurement data are expressed as mean ± SD. * $p < 0.05$, ** $p < 0.01$, *** $p < 0.001$. Sevo, sevoflurane; Ctrl, Control.

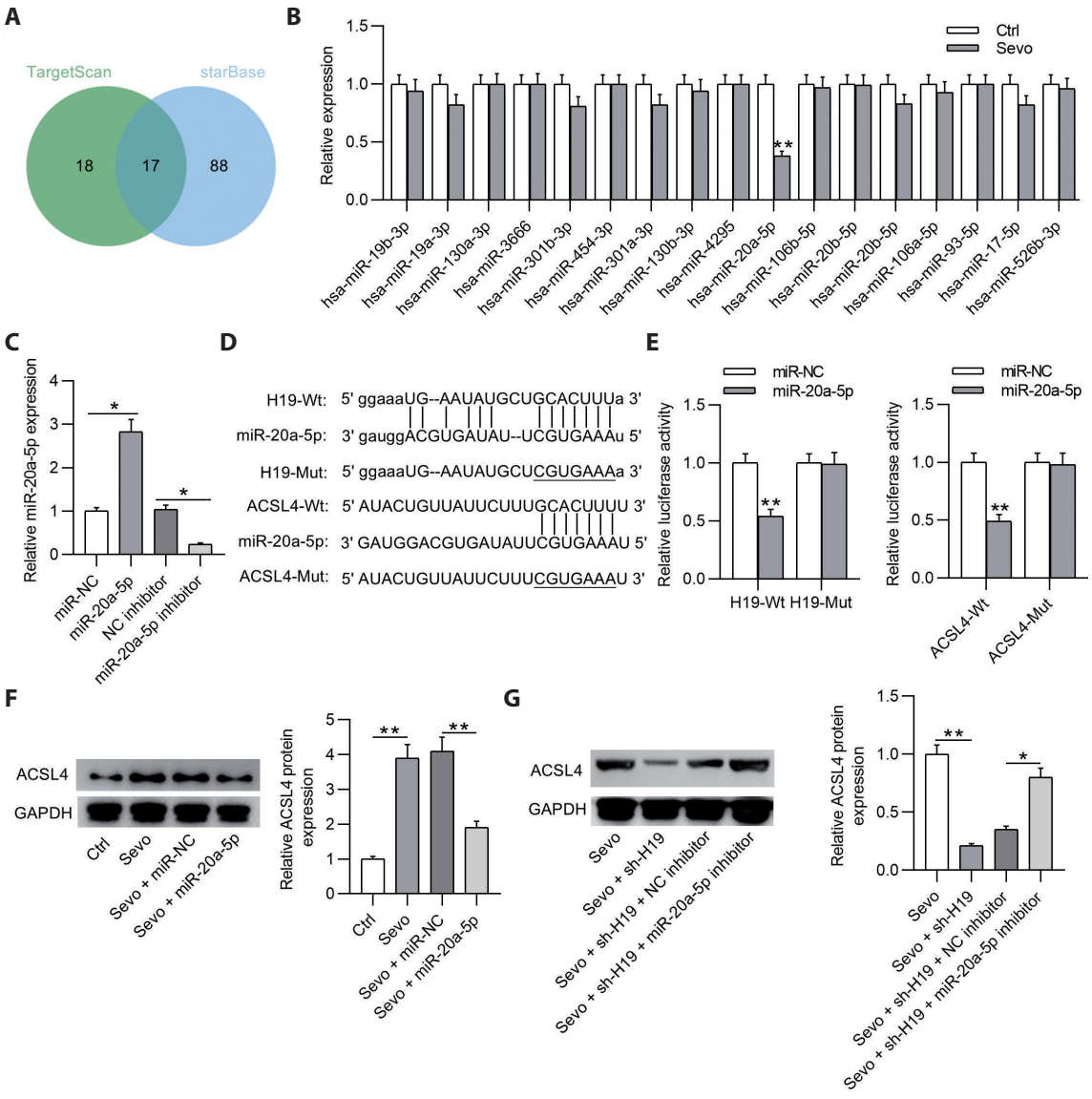
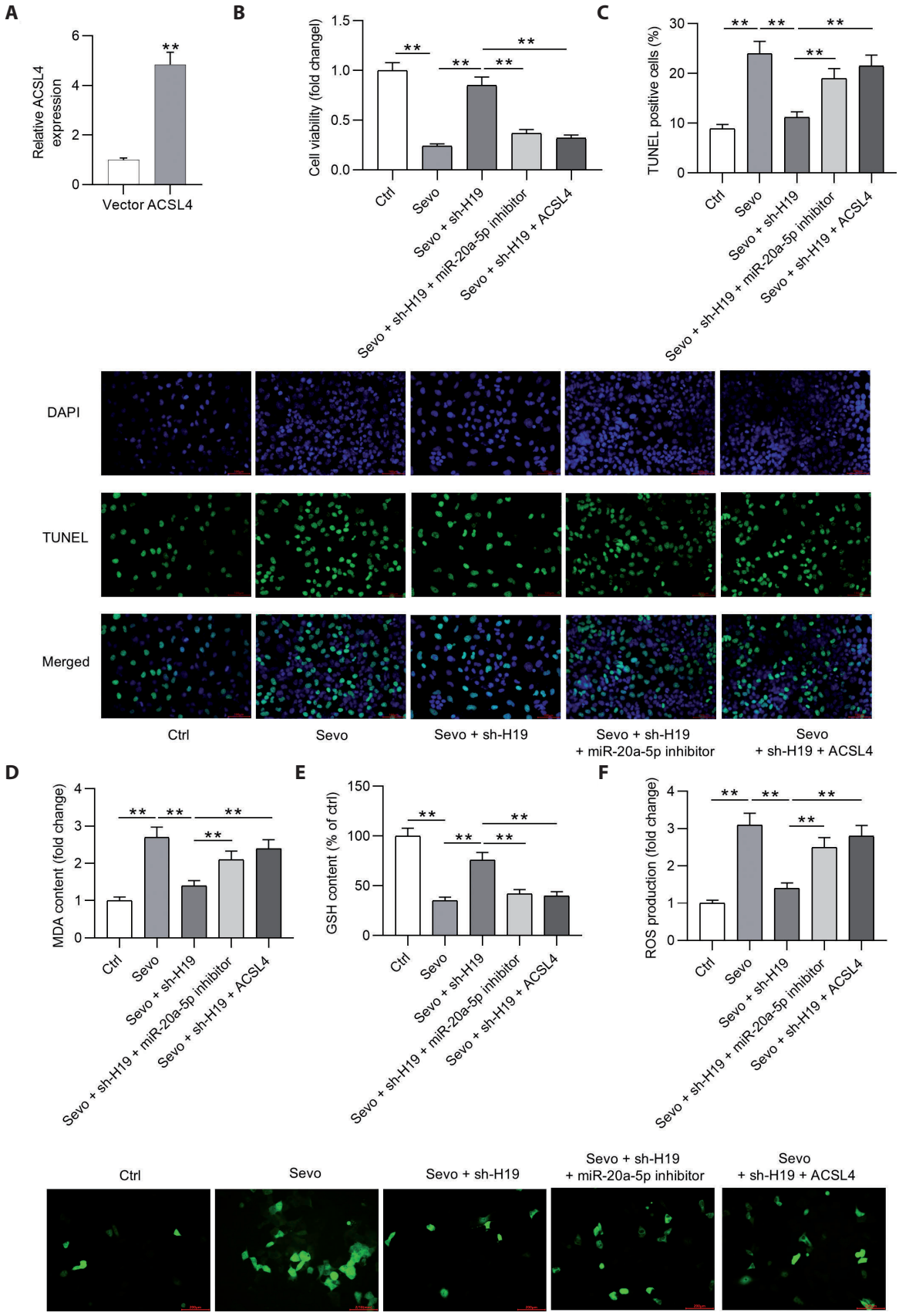


Figure 3. H19 targets ACSL4 *via* sequestration of miR-20a-5p. **A.** ENCORI and TargetScan databases were searched to identify the mutual miRNAs for H19 and ACSL4. **B.** RT-qPCR detected the expression of predicated miRNAs in SH-SY5Y cells exposed to sevoflurane. **C.** The overexpression and knockdown efficiency of miR-20a-5p by RT-qPCR. **D.** The complementary sequences between miR-20a-5p and H19 or ACSL4 as well as the mutated sequences of H19 and ACSL4 were displayed. **E.** Relative luciferase activity of H19-Wt/Mut and ACSL4-Wt/Mut in cells overexpressing miR-20a-5p. **F.** The effects of sevoflurane alone or sevoflurane plus overexpressed miR-20a-5p on ACSL4 expression. **G.** The effects of sh-H19 or miR-20a-5p inhibitor on ACSL4 expression in sevoflurane-treated cells was detected by Western blot analysis. Measurement data are expressed as mean ± SD. * $p < 0.05$, ** $p < 0.01$. Sevo, sevoflurane; Ctrl, Control.


A
Relative ACSL4 expression
Vector ACSL4
B
Cell viability (fold change)
C
TUNEL positive cells (%)
Ctrl
Sevo
Sevo + sh-H19
Sevo + sh-H19 + miR-20a-5p inhibitor
Sevo + sh-H19 + ACSL4
DAPI
TUNEL
Merged
Ctrl
Sevo
Sevo + sh-H19
Sevo + sh-H19 + miR-20a-5p inhibitor
Sevo + sh-H19 + ACSL4
D
MDA content (fold change)
E
GSH content (% of ctrl)
F
ROS production (fold change)
Ctrl
Sevo
Sevo + sh-H19
Sevo + sh-H19 + miR-20a-5p inhibitor
Sevo + sh-H19 + ACSL4

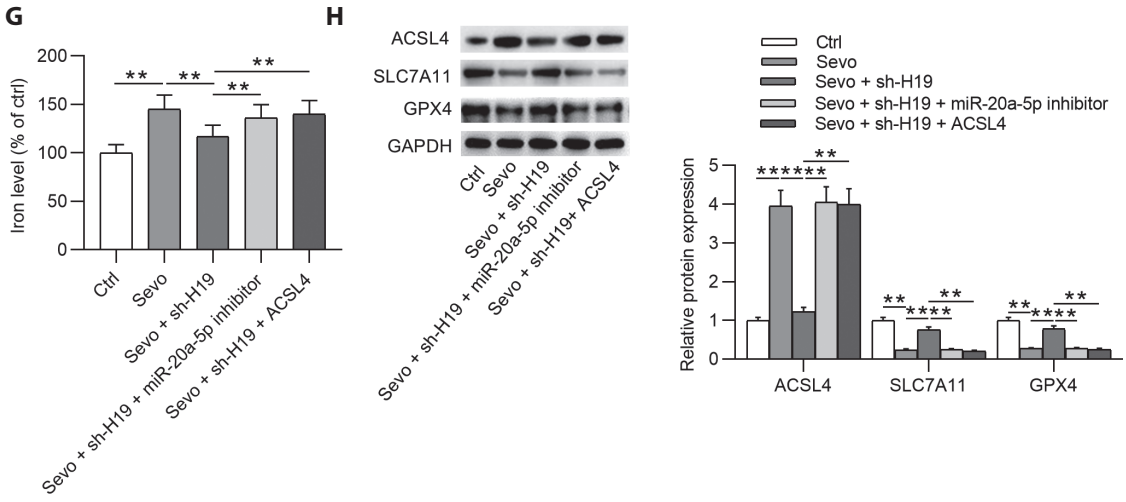


Figure 4. H19 modulates sevoflurane-induced cytotoxicity by targeting the miR-20a-5p/ACSL4 axis. **A.** ACSL4 expression in SH-SY5Y cells transfected with pcDNA3.1/ACSL4. **B.** Cell viability was detected in Ctrl, Sevo, Sevo+sh-H19, Sevo+sh-H19+miR-20a-5p inhibitor, and Sevo+sh-H19+ACSL4 groups by CCK-8 assay. **C.** TUNEL positive cell percentage. Commercial kits examined the contents of MDA (**D**) and GSH (**E**) in the indicated groups. **F.** DCFDA staining assay was performed to test ROS content. **G.** Commercial kits for iron level. **H.** The protein intensity and quantification of ACSL4, SLC7A11, and GPX4 by Western blot analysis. Measurement data are expressed as mean ± SD. ** $p < 0.01$. Sevo, sevoflurane; Ctrl, Control.

by miR-20a-5p and suppressed by miR-20a-5p inhibitor (Fig. 3C). The interacting sequences on H19 and ACSL4 for miR-20a-5p and the mutated sequences were generated for luciferase reporter assay (Fig. 3D). Results delineated that overexpression of miR-20a-5p resulted in the diminishment of luciferase activity on H19-Wt and ACSL4-Wt instead of H19-Mut and ACSL4-Mut (Fig. 3E). Subsequent Western blot analysis demonstrated that sevoflurane-induced ACSL4 protein expression was abrogated by elevated miR-20a-5p (Fig. 3F). In addition, sh-H19-suppressed ACSL4 expression was restored by miR-20a-5p inhibitor in sevoflurane-treated SH-SY5Y cells (Fig. 3G). All these results revealed that H19 targets ACSL4 by sequestrating miR-20a-5p.

H19 targets miR-20a-5p/ACSL4 axis to regulate sevoflurane-induced cytotoxicity

To assess the role of the H19/miR-20a-5p/ACSL4 axis in sevoflurane-induced neuronal damage in SH-SY5Y cells, ACSL4 expression was first enhanced for the follow-up rescue experiments (Fig. 4A). The inductive effect of H19 deficiency on the viability of sevoflurane-induced cells was counteracted by miR-20a-5p inhibitor or ACSL4 (Fig. 4B). Meanwhile, the repressive effect of silenced H19 on the apoptosis of cells exposure to sevoflurane was attenuated by miR-20a-5p knockdown or ACSL4 elevation (Fig. 4C). Under the treatment of sevoflurane, sh-H19-reduced MDA content and -upregulated GSH content were countered upon miR-20a-5p inhibition or ACSL4 overexpression (Fig. 4D,E). Both the ROS production and iron level decreased by depleted H19 was recovered by miR-20a-5p inhibitor or ACSL4 in sevoflurane-exposed cells (Fig. 4F,G). Moreover, knocking down miR-20a-5p or overexpressing ACSL4 reversed sh-H19 transfection-reduced ACSL4 protein expression and H19 silencing-induced expression of SLC7A11 and GPX4 under sevoflurane stimulation (Fig. 4H). In a word, elevated ACSL4 reverses sh-H19-attenuated cytotoxicity of sevoflurane-treated SH-SY5Y cells.

Discussion

More and more attention has been paid to the toxic effects of anesthetic drugs on neurons and the consequent persistent cognitive deficit (Verlinde et al. 2016; Ho et al. 2017). It is well concerned that a link between neurotoxicity generated by anesthetic drugs and cell death mechanisms, especially ferroptosis, has been highlighted. High levels of the accumulated iron have been found to evoke neurotoxicity and serious cognitive impairment (Masaldan et al. 2019). An *in vitro* study reveals that isoflurane administration impairs GPX4 expression, mitochondrial transmembrane potential, and fortifies ROS generation, finally resulting in neuronal death. In addition, isoflurane-induced toxic effect on primary cortical neurons *in vivo* can be ameliorated by Fer-1 pretreatment (Xia et al. 2018). Furthermore, isoflurane-stimulated SH-SY5Y cells display the phosphorylated Bcl-1 and the Beclin 1-solute carrier family 7-member 11 com-

plex, which thus aggravate isoflurane-triggered ferroptotic neuronal death (Liu et al. 2019). This evidence reveals that ferroptosis is one of the pivotal mechanisms involving anesthetics-generated neurotoxicity. Therefore, suppressing ferroptotic neuronal death might become an effective therapeutic strategy for mitigating anesthetic drug-caused nerve injury and secondary brain injury. In this study, we observed that sevoflurane impaired SH-SY5Y cell viability in a time-dependent manner. Additionally, 4.1% sevoflurane time dependently upregulated Bax expression and iron level, whereas decreased Bcl-2, SLC7A11 and GPX4 expression in SH-SY5Y cells.

Accumulating studies demonstrate that aberrant expression of lncRNAs is interrelated with the occurrence of sevoflurane-induced neuronal damage. For example, elevation of lncRNA Gm43050 ameliorates sevoflurane exposure-induced inflammation response and apoptosis in primary hippocampal neurons (Xu W et al. 2020). The lncRNA Neat1 is highly expressed in sevoflurane-induced HT22 cells, and silencing of Neat1 meliorates sevoflurane-triggered neurotoxicity by restoring cell viability and impairing ROS production, neuroinflammation, and cell apoptosis (Wei et al. 2021). Our data verified that H19 promoted SH-SY5Y cell ferroptosis by modulating the miR-20a-5p/ACSL4 axis. Plenty of reports have suggested that H19 is implicated in the pathogenesis of some neurodegenerative diseases (Zhang Y et al. 2020; Li et al. 2021). The specific modulatory function of H19 has also been proved in ankylosing spondylitis, atherosclerosis, and diabetic retinopathy (Pan 2017; Thomas et al. 2019; Zhang X et al. 2020). Additionally, H19 expression is at a high level in isoflurane-induced HT22 cells compared with control cells (Ge et al. 2022), and suppressing H19 inhibits BMVEC ferroptosis in intracerebral hemorrhage (Chen et al. 2021), suggesting that H19 might be a biomarker of anesthetic drug-induced neurotoxicity. Consistently, H19 was upregulated in sevoflurane-treated SH-SY5Y cell line, and depletion of H19 recovered cell viability and suppressed ferroptosis.

Cytoplasm-localized lncRNAs can function as ceRNAs to sponge miRNAs and modulate cellular processes by decreasing their expression. To probe into the explicit mechanism by which H19 regulated sevoflurane-affected SH-SY5Y cellular activities, predictive analysis was conducted, and we found that miR-20a-5p was a target miRNA for H19. A recent study indicates that overexpressed miR-20a-5p alleviates 1-methyl-4-phenyl pyridine ion-induced neurotoxicity by attenuating cell damage, inflammation, and mitochondrial dysfunction in Parkinson's disease (Wang et al. 2021). Silenced miR-20a-5p hinders neuronal branching and axonal growth and inhibits epileptogenesis *via* synaptic plasticity mediated by RGMa-RhoA (Feng et al. 2020). Nevertheless, the role of miR-20a-5p has not been explored in sevoflurane-induced neurons. Our study showed that miR-20a-5p was downregulated after sevoflurane exposure and it was combined by H19. Most importantly, miR-20a-5p inhibitor reversed H19 silencing-restored cell viability and H19 knockdown-attenuated ferroptosis.

To further develop the ceRNA hypothesis, the downstream target mRNAs of miR-20a-5p was searched and ACSL4 was identified through bioinformatics analysis. By performing luciferase reporter assay, miR-20a-5p was verified to combine with ACSL4. To date, the essential function of ACSL4 has been well proved in ferroptosis (Kebaili et al. 1994). It has been reported that ischemia reperfusion-

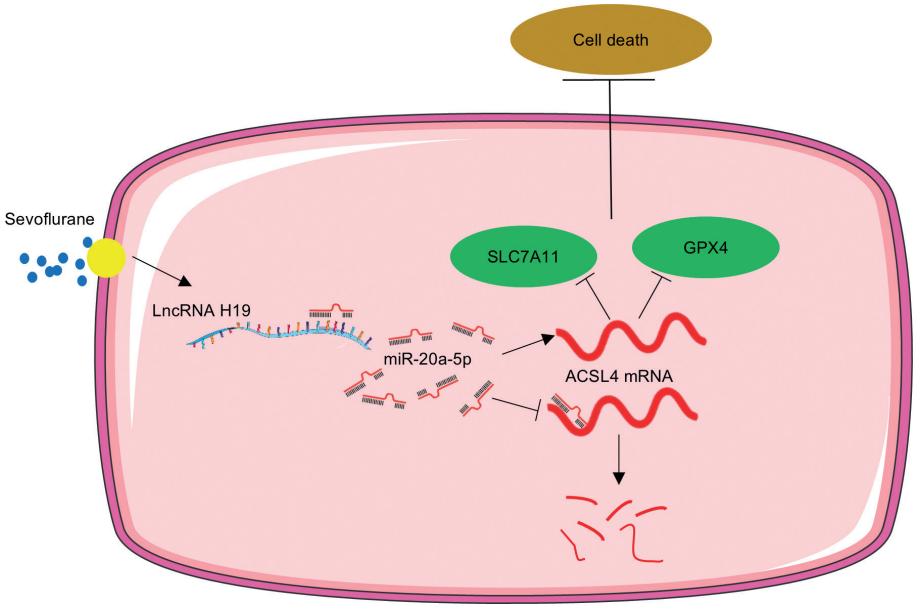


Figure 5. LncRNA H19 was highly expressed in sevoflurane-induced SH-SY5Y cells, and it elevated ACSL4 expression by inhibiting miR-20a-5p expression through a ceRNA mechanism. Then, the upregulated ACSL4 inhibited SLC7A11 and GPX4 expression to facilitate neuron death through ferroptosis.

generated lung injury is mitigated by restraining ferroptosis *via* inhibition of ACSL4 to elevate GPX4 and GSH expression and reduce lipid peroxidation (Xu Y et al. 2020). The brain tissues of subarachnoid hemorrhage (SAH) rat models exhibit elevated ACSL4 expression; either ferroptosis suppression or ACSL4 deficiency alleviates neuronal damage caused by SAH, suggesting that ACSL4 knockdown attenuates SAH-induced early brain injury *via* restraining ferroptosis (Qu et al. 2021). Notably, ACSL4 is upregulated after sevoflurane treatment and neuronal cell death induced by sevoflurane induction is eliminated by silenced ACSL4 as manifested by the enhanced cell viability, GPX4, and GSH levels and the reduced MDA content, ROS generation, and iron levels (Cheng et al. 2021). Consistently, ACSL4 expression was also increased in sevoflurane-stimulated SH-SY5Y cells. Both overexpression of miR-20a-5p and knockdown of H19 suppressed ACSL4 expression in sevoflurane-induced SH-SY5Y cells. Most importantly, ACSL4 expression reduced by silenced H19 was restored by inhibition of miR-20a-5p, implying that H19 targets ACSL4 *via* sequestration of miR-20a-5p. Rescue experiments illuminated that the enhanced cell viability and the attenuated ferroptosis in H19-silenced SH-SY5Y cells were reversed by elevation of ACSL4.

In summary, H19 reduction protected against sevoflurane exposure-induced ferroptosis *via* regulation of the miR-20a-5p/ACSL4 axis (Fig. 5). Thus, the H19/miR-20a-5p/ACSL4 axis might represent a potential therapeutic target for treating sevoflurane or other anesthetic drugs-induced neurotoxicity and secondary brain injury. However, there were several limitations in our investigation. First, the protective role of reduced H19 in sevoflurane-induced SH-SY5Y cells was just validated by *in vitro* experiments, and *in vivo* assays are needed to further determine whether H19 inhibition exerts protective function in sevoflurane-induced animal models. Second, due to the complexity of molecular mechanisms, the upstream molecules or downstream signaling pathways of the H19/miR-20a-5p/ACSL4 axis still need further exploration.

Ethics approval. This article does not contain any studies on human or animal subjects.

Acknowledgement. We appreciate the support of First Hospital of Jilin University.

Conflicts of interest. The authors declare that there are no competing interests in this study.

Contributions of authors. LL conceived and designed the experiments. LL, ZX, Yan L and Ying L carried out the experiments. LL and Ying L analyzed the data. LL and Ying L drafted the manuscript. All authors agreed to be accountable for all aspects of the work. All authors have read and approved the final manuscript.

Data availability statement. Data will be made available on reasonable request.

References

Bai RX, Tang ZY (2021): Long non-coding RNA H19 regulates Bcl-2, Bax and phospholipid hydroperoxide glutathione peroxidase expression in spontaneous abortion. Exp. Ther. Med. **21,** 41 https://doi.org/10.3892/etm.2020.9473

Chen B, Wang H, Lv C, Mao C, Cui Y (2021): Long non-coding RNA H19 protects against intracerebral hemorrhage injuries via regulating microRNA-106b-5p/acyl-CoA synthetase long chain family member 4 axis. Bioengineered **12,** 4004-4015 https://doi.org/10.1080/21655979.2021.1951070

Cheng J, Fan YQ, Liu BH, Zhou H, Wang JM, Chen QX (2020): ACSL4 suppresses glioma cells proliferation via activating ferroptosis. Oncol. Rep. **43,** 147-158 https://doi.org/10.3892/or.2019.7419

Cheng L, Zhu X, Liu Y, Zhu K, Lin K, Li F (2021): ACSL4 contributes to sevoflurane-induced ferroptotic neuronal death in SH-SY5Y cells via the 5' AMP-activated protein kinase/mammalian target of rapamycin pathway. Ann. Transl. Med. **9,** 1454 https://doi.org/10.21037/atm-21-4249

Cui Y, Zhang Y, Zhao X, Shao L, Liu G, Sun C, Xu R, Zhang Z (2021): ACSL4 exacerbates ischemic stroke by promoting ferroptosis-induced brain injury and neuroinflammation. Brain Behav. Immun. **93,** 312-321 https://doi.org/10.1016/j.bbi.2021.01.003

Dieter C, Lourenco ED, Lemos NE (2020): Association of long non-coding RNA and leukemia: A systematic review. Gene **735,** 144405 https://doi.org/10.1016/j.gene.2020.144405

Doll S, Proneth B, Tyurina YY, Panzilius E, Kobayashi S, Ingold I, Irmler M, Beckers J, Aichler M, Walch A, et al. (2017): ACSL4 dictates ferroptosis sensitivity by shaping cellular lipid composition. Nat. Chem. Biol. **13,** 91-98 https://doi.org/10.1038/nchembio.2239

Dong Y, Zhang G, Zhang B, Moir RD, Xia W, Marcantonio ER, Culley DJ, Crosby G, Tanzi RE, Xie Z (2009): The common inhalational anesthetic sevoflurane induces apoptosis and increases beta-amyloid protein levels. Arch. Neurol. **66,** 620-631 https://doi.org/10.1001/archneurol.2009.48

Feng Y, Duan C, Luo Z, Xiao W, Tian F (2020): Silencing miR-20a-5p inhibits axonal growth and neuronal branching and prevents epileptogenesis through RGMa-RhoA-mediated synaptic plasticity. J. Cell Mol. Med. **24,** 10573-10588 https://doi.org/10.1111/jcmm.15677

Ge Y, Lin D, Cui B, Zhang L, Li S, Wang Z, Ma J (2022): Effects of long noncoding RNA H19 on isoflurane-induced cognitive dysregulation by promoting neuroinflammation. Neuroimmunomodulation **29,** 117-127 https://doi.org/10.1159/000519124

Geng JF, Liu X, Zhao HB, Fan WF, Geng JJ, Liu XZ (2018): LncRNA UCA1 inhibits epilepsy and seizure-induced brain injury by regulating miR-495/Nrf2-ARE signal pathway. Int. J. Biochem. Cell Biol. **99,** 133-139 https://doi.org/10.1016/j.biocel.2018.03.021

Hirschhorn T, Stockwell BR (2019): The development of the concept of ferroptosis. Free Radic. Biol. Med. **133,** 130-143 https://doi.org/10.1016/j.freeradbiomed.2018.09.043

Ho AM, Fleming ML, Mizubuti GB (2017): Anesthetic neurotoxicity and the developing brain. CMAJ **189,** E1028-1029 https://doi.org/10.1503/cmaj.170313

Kagan VE, Mao G, Qu F, Angeli JP, Doll S, Croix CS, Dar HH, Liu B, Tyurin VA, Ritov VB, et al. (2017): Oxidized arachidonic and adrenic PEs navigate cells to ferroptosis. Nat. Chem. Biol. **13,** 81-90 https://doi.org/10.1038/nchembio.2238

Kebaili K, Bertrand Y, Foray P, Taylor P, Combet S, Berthier JC, Pangaud N, Philippe N (1994): A rare cause of hyponatremia during introductory treatment of acute lymphoblastic leukemia in an infant: inappropriate secretion of atrial natriuretic factor? Arch. Pediatr. **1,** 898-902

Kim JM, Moon J, Yu JS, Park DK, Lee ST, Jung KH, Chu K (2019): Altered long noncoding RNA profile after intracerebral hemorrhage. Ann. Clin. Transl. Neurol. **6,** 2014-2025 https://doi.org/10.1002/acn3.50894

Kodama M, Satoh Y, Otsubo Y, Araki Y, Yonamine R, Masui K, Kazama T (2011): Neonatal desflurane exposure induces more robust neuroapoptosis than do isoflurane and sevoflurane and impairs working memory. Anesthesiology **115,** 979-991 https://doi.org/10.1097/ALN.0b013e318234228b

Kuwata H, Hara S (2019): Role of acyl-CoA synthetase ACSL4 in arachidonic acid metabolism. Prostaglandins Other Lipid Mediat. **144,** 106363 https://doi.org/10.1016/j.prostaglandins.2019.106363

Lai Z, Zhang L, Su J, Cai D, Xu Q (2016): Sevoflurane postconditioning improves long-term learning and memory of neonatal hypoxia-ischemia brain damage rats via the PI3K/Akt-mPTP pathway. Brain Res. **1630,** 25-37 https://doi.org/10.1016/j.brainres.2015.10.050

Le Freche H, Brouillette J, Fernandez-Gomez FJ, Patin P, Caillierez R, Zommer N, Sergeant N, Buée-Scherrer V, Lebuffe G, Blum D, et al. (2012): Tau phosphorylation and sevoflurane anesthesia: an association to postoperative cognitive impairment. Anesthesiology **116,** 779-787 https://doi.org/10.1097/ALN.0b013e31824be8c7

Li X, Qian Y, Tang K, Li Y, Tao R, Gong C, Huang L, Zou K, Liu L (2021): Inhibition of lncRNA H19/miR-370-3p pathway mitigates neuronal apoptosis in an in vitro model of spinal cord injury (SCI). Transl. Neurosci. **12,** 103-113 https://doi.org/10.1515/tnsci-2021-0013

Liu NX, Li QH (2020): LncRNA BC200 regulates neuron apoptosis and neuroinflammation via PI3K/AKT pathway in Alzheimer's disease. J. Biol. Regul. Homeost. Agents **34,** 2255-2261 https://doi.org/10.23812/20-498-L

Liu R, Li X, Zhao G (2019): Beclin1-mediated ferroptosis activation is associated with isoflurane-induced toxicity in SH-SY5Y neuroblastoma cells. Acta Biochim. Biophys. Sin. (Shanghai) **51,** 1134-1141 https://doi.org/10.1093/abbs/gmz104

Liu Y, Wu G (2020): NNT-AS1 enhances bladder cancer cell growth by targeting miR-1301-3p/PODXL axis and activating Wnt pathway. Neurourol. Urodyn. **39,** 547-557 https://doi.org/10.1002/nau.24238

Lu Y, Huang Y, Jiang J, Hu R, Yang Y, Jiang H, Yan J (2016): Neuronal apoptosis may not contribute to the long-term cognitive dysfunction induced by a brief exposure to 2% sevoflurane in developing rats. Biomed. Pharmacother. **78,** 322-328 https://doi.org/10.1016/j.biopha.2016.01.034

Ma N, Tie C, Yu B, Zhang W, Wan J (2020): Identifying lncRNA-miRNA-mRNA networks to investigate Alzheimer's disease pathogenesis and therapy strategy. Aging (Albany NY) **12,** 2897-2920 https://doi.org/10.18632/aging.102785

Masaldan S, Bush AI, Devos D, Rolland AS, Moreau C (2019): Striking while the iron is hot: Iron metabolism and ferroptosis in neurodegeneration. Free Radic. Biol. Med. **133,** 221-233 https://doi.org/10.1016/j.freeradbiomed.2018.09.033

Meng L, Zhang Y, He X, Hu C (2022): LncRNA H19 modulates neuropathic pain through miR-141/GLI2 axis in chronic constriction injury (CCI) rats. Transpl. Immunol. **71,** 101526 https://doi.org/10.1016/j.trim.2021.101526

Pan JX (2017): LncRNA H19 promotes atherosclerosis by regulating MAPK and NF-kB signaling pathway. Eur. Rev. Med. Pharmacol. Sci. **21,** 322-328

Pouyanrad S, Rahgozar S, Ghodousi ES (2019): Dysregulation of miR-335-3p, targeted by NEAT1 and MALAT1 long noncoding RNAs, is associated with poor prognosis in childhood acute lymphoblastic leukemia. Gene **692,** 35-43 https://doi.org/10.1016/j.gene.2019.01.003

Qu XF, Liang TY, Wu DG, Lai NS, Deng RM, Ma C, Li X, Li HY, Liu YZ, Shen HT, et al. (2021): Acyl-CoA synthetase long chain family member 4 plays detrimental role in early brain injury after subarachnoid hemorrhage in rats by inducing ferroptosis. CNS Neurosci. Ther. **27,** 449-463 https://doi.org/10.1111/cns.13548

Ramos AD, Diaz A, Nellore A, Delgado RN, Park KY, Gonzales-Roybal G, Oldham MC, Song JS, Lim DA (2013): Integration of genome-wide approaches identifies lncRNAs of adult neural stem cells and their progeny in vivo. Cell Stem Cell. **12,** 616-628 https://doi.org/10.1016/j.stem.2013.03.003

Sánchez-Conde P, Rodríguez-López JM, Nicolás JL, Lozano FS, García-Criado FJ, Cascajo C, González-Sarmiento R, Muriel C (2008): The comparative abilities of propofol and sevoflurane to modulate inflammation and oxidative stress in the kidney after aortic cross-clamping. Anesth. Analg. **106,** 371-378 https://doi.org/10.1213/ane.0b013e318160580b

Shi X, Wei YT, Li H, Jiang T, Zheng XL, Yin K, Zhao GJ (2020): Long non-coding RNA H19 in atherosclerosis: what role? Mol. Med. **26,** 72 https://doi.org/10.1186/s10020-020-00196-w

Thomas AA, Biswas S, Feng B, Chen S, Gonder J, Chakrabarti S (2019): lncRNA H19 prevents endothelial-mesenchymal transition in diabetic retinopathy. Diabetologia **62,** 517-530 https://doi.org/10.1007/s00125-018-4797-6

Tian Y, Guo S, Wu X, Ma L, Zhao X (2015): Minocycline alleviates sevoflurane-induced cognitive impairment in aged rats. Cell. Mol. Neurobiol. **35,** 585-594 https://doi.org/10.1007/s10571-014-0154-6

Verlinde M, Hollmann MW, Stevens MF, Hermanns H, Werdehausen R, Lirk P (2016): Local anesthetic-induced neurotoxicity. Int. J. Mol. Sci. **17,** 339

https://doi.org/10.3390/ijms17030339
Wang Q, Wang Y, Zhou F, Li J, Lu G, Zhao Y (2021): MiR-20a-5p regulates MPP(+)-induced oxidative stress and neuroinflammation in HT22 cells by targeting IRF9/NF-κB axis. Evid. Based Complement. Alternat. Med. **2021,** 6621206
https://doi.org/10.1155/2021/6621206
Wei X, Xu S, Chen L (2021): LncRNA Neat1/miR-298-5p/Srpk1 contributes to sevoflurane-induced neurotoxicity. Neurochem. Res. **46,** 3356-3364
https://doi.org/10.1007/s11064-021-03436-5
Wu J, Yang JJ, Cao Y, Li H, Zhao H, Yang S, Li K (2020): Iron overload contributes to general anaesthesia-induced neurotoxicity and cognitive deficits. J. Neuroinflammation **17,** 110
https://doi.org/10.1186/s12974-020-01777-6
Wu Y, Song J, Wang Y, Wang X, Culmsee C, Zhu C (2019): The potential role of ferroptosis in neonatal brain injury. Front. Neurosci. **13,** 115
https://doi.org/10.3389/fnins.2019.00115
Xia Y, Sun X, Luo Y, Stary CM (2018): Ferroptosis contributes to isoflurane neurotoxicity. Front. Mol. Neurosci. **11,** 486
https://doi.org/10.3389/fnmol.2018.00486
Xu W, Zhao Y, Ai Y (2020): Overexpression of lncRNA Gm43050 alleviates apoptosis and inflammation response induced by sevoflurane treatment by regulating miR-640/ZFP91. Am. J. Transl. Res. **12,** 4337-4346
Xu Y, Li X, Cheng Y, Yang M, Wang R (2020): Inhibition of ACSL4 attenuates ferroptotic damage after pulmonary ischemia-reperfusion. FASEB J. **34,** 16262-16275
https://doi.org/10.1096/fj.202001758R
Yuan H, Li X, Zhang X, Kang R, Tang D (2016): Identification of ACSL4 as a biomarker and contributor of ferroptosis. Biochem. Biophys. Res. Commun. **478,** 1338-1343
https://doi.org/10.1016/j.bbrc.2016.08.124
Zhang B, Chen J, Cui M, Jiang Y (2020): LncRNA ZFAS1/miR-1271-5p/HK2 promotes glioma development through regulating proliferation, migration, invasion and apoptosis. Neurochem. Res. **45,** 2828-2839
https://doi.org/10.1007/s11064-020-03131-x
Zhang J, Wang R (2021): Deregulated lncRNA MAGI2-AS3 in Alzheimer's disease attenuates amyloid-β induced neurotoxicity and neuroinflammation by sponging miR-374b-5p. Exp. Gerontol. **144,** 111180
https://doi.org/10.1016/j.exger.2020.111180
Zhang X, Ji S, Cai G, Pan Z, Han R, Yuan Y, Xu S, Yang J, Hu X, Chen M, et al. (2020): H19 increases IL-17A/IL-23 releases via regulating VDR by interacting with miR675-5p/miR22-5p in ankylosing spondylitis. Mol. Ther. Nucleic Acids **19,** 393-404
https://doi.org/10.1016/j.omtn.2019.11.025
Zhang Y, Xia Q, Lin J (2020): LncRNA H19 attenuates apoptosis in MPTP-induced Parkinson's disease through regulating miR-585-3p/PIK3R3. Neurochem. Res. **45,** 1700-1710
https://doi.org/10.1007/s11064-020-03035-w
Zhu G, Tao L, Wang R, Xue Y, Wang X, Yang S, Sun X, Gao G, Mao Z, Yang Q (2017): Endoplasmic reticulum stress mediates distinct impacts of sevoflurane on different subfields of immature hippocampus. J. Neurochem. **142,** 272-285
https://doi.org/10.1111/jnc.14057
Zuo Y, Chang Y, Thirupathi A, Zhou C, Shi Z (2021): Prenatal sevoflurane exposure: Effects of iron metabolic dysfunction on offspring cognition and potential mechanism. Int. J. Dev. Neurosci. **81,** 1-9
https://doi.org/10.1002/jdn.10080

Received: April 23, 2025
Final version accepted: May 26, 2025